Electronic Supplementary Material (ESI) for New Journal of Chemistry.

Supporting information

Fluorescence 'off-on-off' signaling with Zinc ensemble: A new array of investigating prevalence of ATP in liver cancer cells

Shampa Kundu[a], Md Majharul Islam[b], Sukhendu Mandal[b] and Prithidipa Sahoo[a]*

[a]Department of Chemistry, Visva-Bharati University, Santiniketan-731235, India
Email: prithidipa@hotmail.com

[b]Department of Microbiology, University of Calcutta, Kolkata-700073, India

1. NMR Studies:

^{1}H NMR of NPAC in DMSO-d_6 :

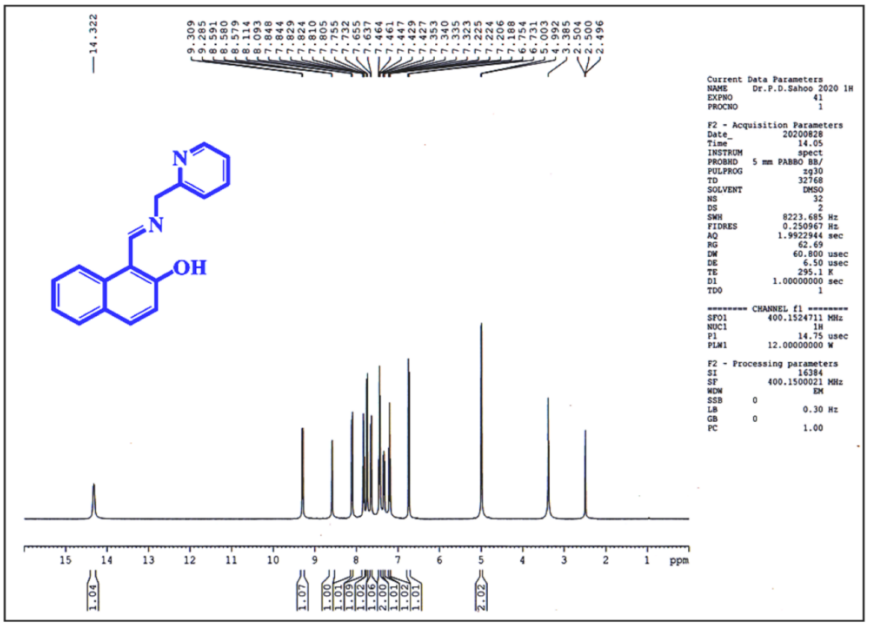

Fig. S1. ^{1}H NMR of **NPAC** in DMSO-d_6 (400 MHz).

^{13}C NMR of NPAC in DMSO-d_6:

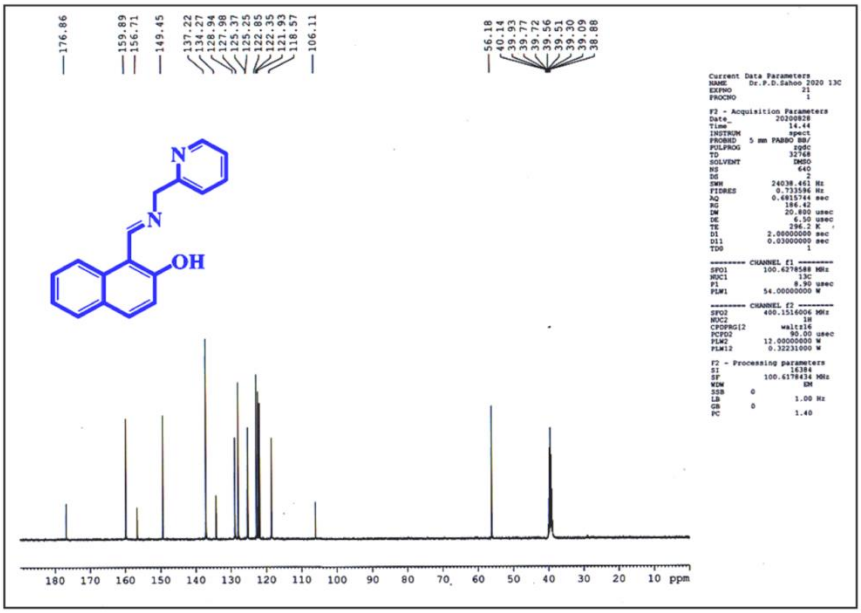

Fig. S2 ^{13}C NMR of **NPAC** in DMSO-d_6 (400 MHz).

2. ^{13}C NMR titration spectrum of NPAC with Zn^{2+} & ATP :

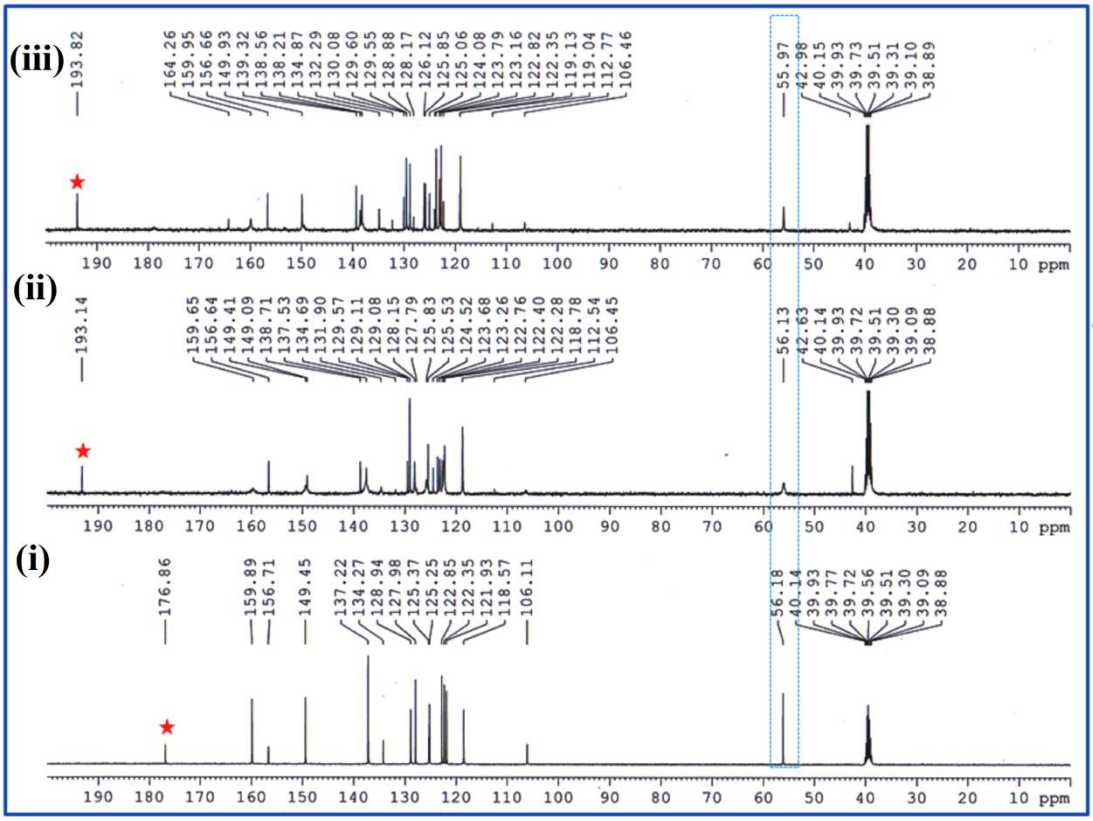

Fig. S3 ^{13}C NMR titration [400MHz] of **NPAC** in DMSO-d_6 at 25^0C and the corresponding changes after consecutive addition of Zn^{2+} & ATP in D_2O where (i) only **NPAC** (ii) **NPAC** + 0.5 equiv. of Zn^{2+}, (iii) [**NPAC-Zn^{2+}] +** 1 equiv. of ATP.

3. Partial HRMS of the mixed assay system:

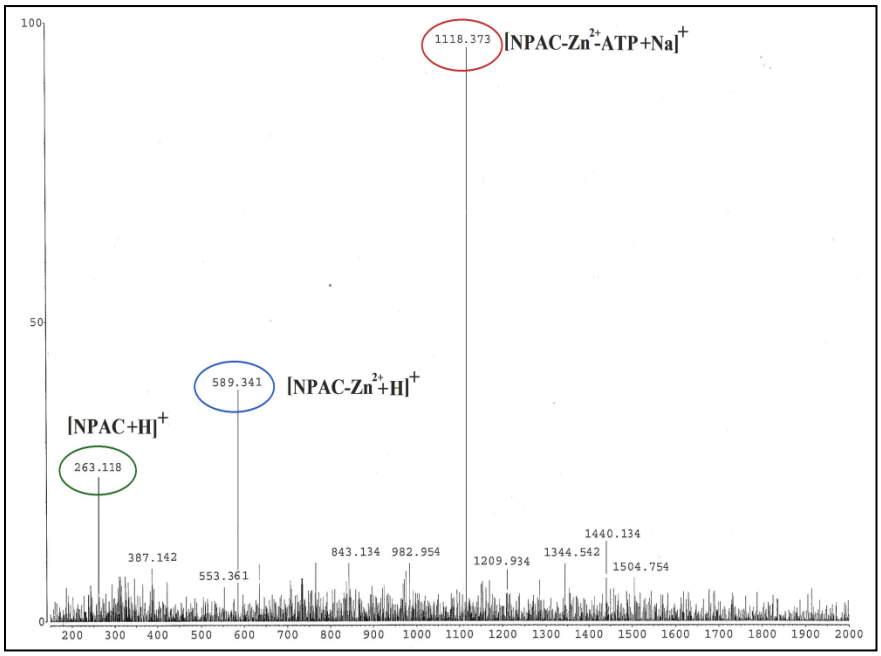

Fig. S4. Partial HRMS spectra of [**NPAC-Zn^{2+}-ATP]** mixture in acetonitrile.

4. Absorbance & Fluorescence study of NPAC with Zn^{2+}:

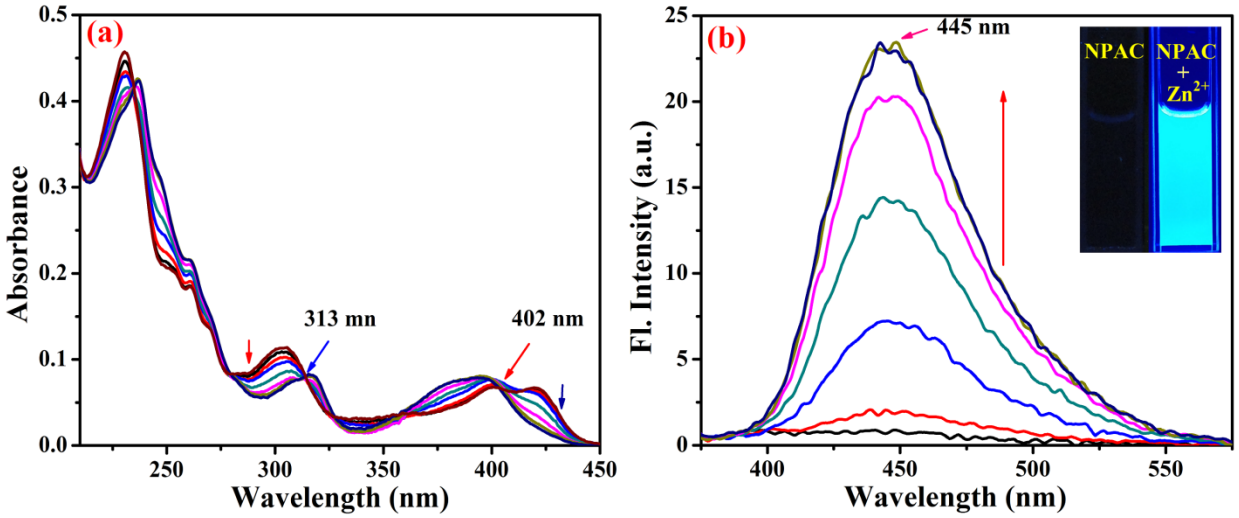

Fig. S5 UV−vis absorption spectra of **NPAC** (1 μM) upon gradual addition of Zn^{2+} up to 0.6 equiv. in CH_3CN:H_2O (1:9, v/v) at pH 7.0 (10 mM phosphate buffer). (b) Fluorescence emission spectra at 445 nm (λ_{ex} = 350 nm) of **NPAC** (1 μM) upon addition of Zn^{2+} upto 0.6 equiv. in

CH_3CN: H_2O (1:9, v/v) at pH 7.0 (10 mM phosphate buffer). [Inset: Fluorescence color changes of **NPAC** and **NPAC** + Zn^{2+} in neutral aqueous medium].

5. Job's plot for NPAC determining the binding stoichiometry towards Zn^{2+} by fluorescence method:

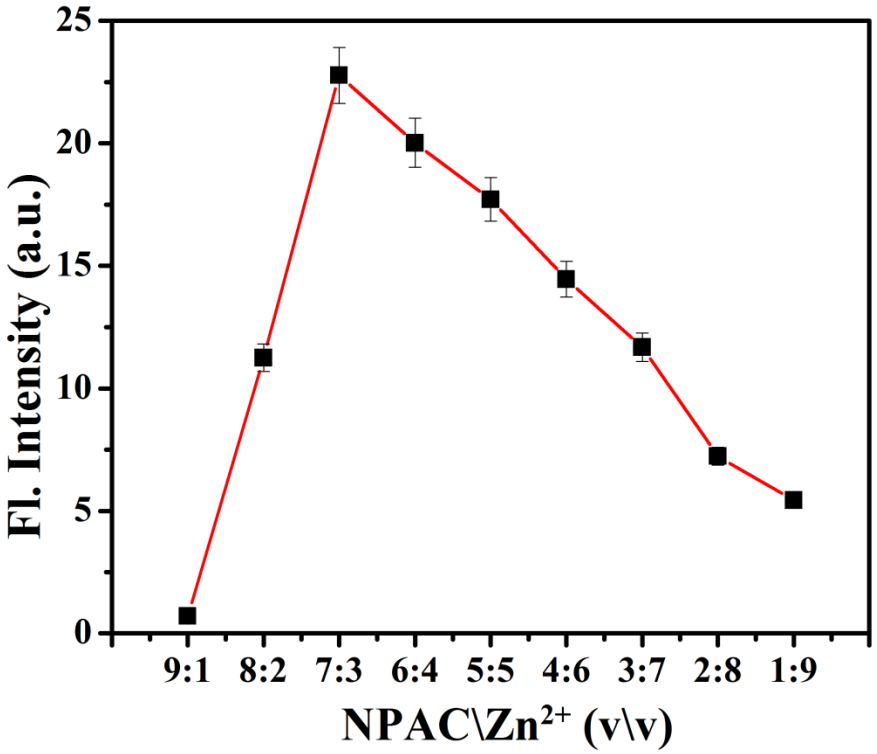

Fig. S6 Job's plot of **NPAC** (c =1µM) with Zn^{2+} (1 µM) in acetonitrile-water (1:9, v/v) at neutral pH (pH 7.0, 10 mM phosphate buffer) by fluorescence method, which indicate 2:1 stoichiometry for **NPAC** with Zn^{2+}. Standard deviations are represented by error bar (n=3).

6. Calculation of binding constants of NPAC towards Zn^{2+}:

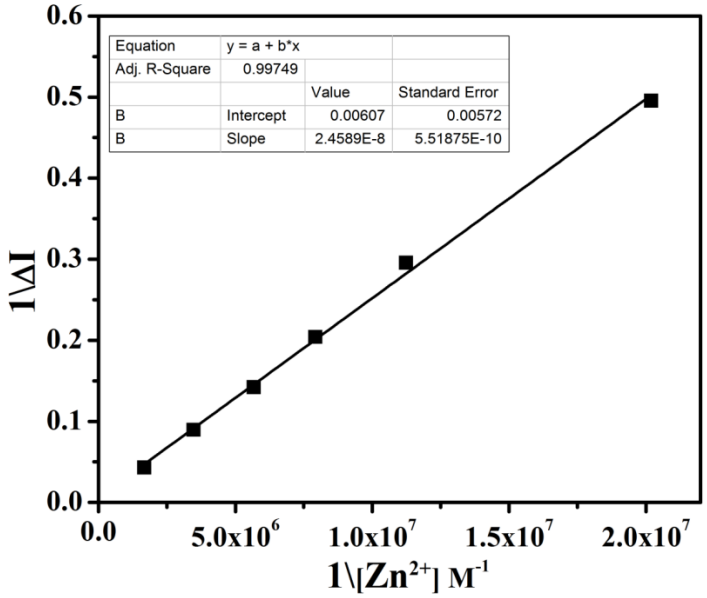

Fig. S7 Linear regression analysis for the calculation of binding constant values of **NPAC** towards Zn^{2+}.

The association const. (K_a) of **NPAC** for sensing Zn^{2+} was determined from the equation: K_a = intercept/slope. From the linear fit graph we get intercept= 0.00607, slope = 2.4589×10^{-8} . Thus we get, $\mathbf{K_a}$ = (0.00607) / (2.4589×10^{-8}) = $\mathbf{0.24 \times 10^6\ M^{-1}}$.

7. Calculation of limit of detection (LOD) of NPAC with Zn^{2+}:

The detection limit of the chemosensor **NPAC** for Zn^{2+} was calculated on the basis of fluorescence titration. To determine the standard deviation for the fluorescence intensity, the emission intensity of four individual receptors without Zn^{2+} was measured by 10 times and the standard deviation of blank measurements was calculated.

The limit of detection (LOD) of **NPAC** for sensing Zn^{2+} was determined from the following equation[1].

$$LOD = K \times SD/S$$

Where K = 2 or 3 (we take 3 in this case); SD is the standard deviation of the blank receptor solution; S is the slope of the calibration curve.

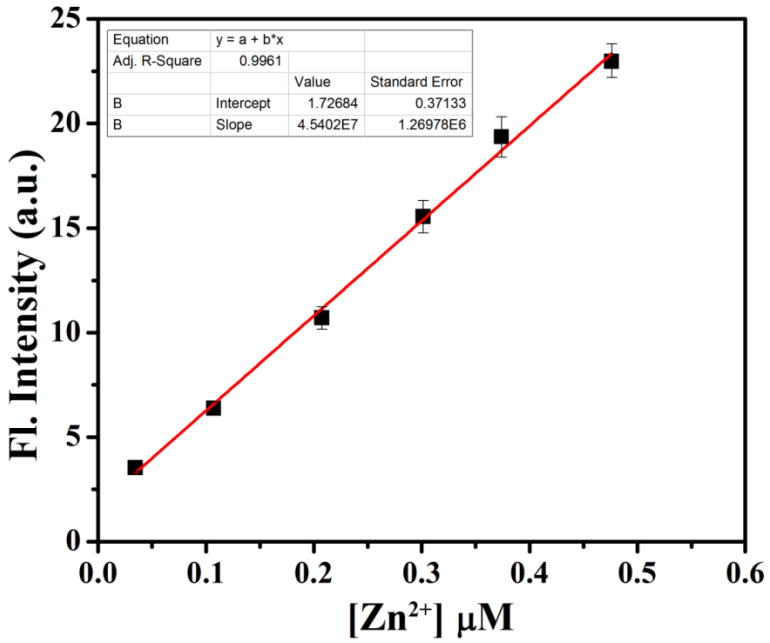

Fig. S8 Linear fit curve of **NPAC** at 445 nm with respect to Zn^{2+} concentration. Standard deviations are represented by error bar (n=3).

From the linear fit graph we get slope = 4.5402× 10^{7}, and SD value is 0.47143. Thus using the above formula we get the Limit of Detection = 0. 31 × 10^{-7} M, i.e 31 nM. Therefore **NPAC** can detect Zn^{2+} up to this very lower concentration by fluorescence technique.

8. Calculation of binding constants of NPAC-Zn^{2+} complex towards ATP:

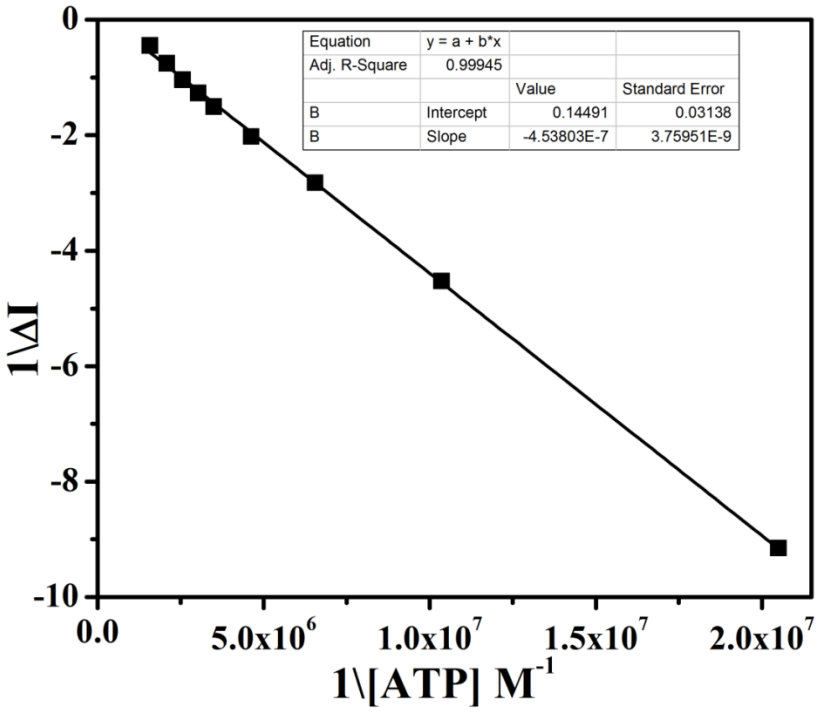

Fig. S9 Linear regression analysis for the calculation of binding constant values of **NPAC-Zn^{2+}** complex towards ATP.

The association const. (K_a) of **NPAC-Zn^{2+}** complex for sensing ATP was determined from the equation: K_a = intercept/slope. From the linear fit graph we get intercept= 0.14491, slope = 4.53803×10^{-7}). Thus we get, $\mathbf{K_a}$ = (0.14491) / 4.53803×10^{-7}) = $\mathbf{0.31 \times 10^6\ M^{-1}}$.

9. Calculation of limit of detection (LOD) of NPAC -Zn^{2+} complex with **ATP:**

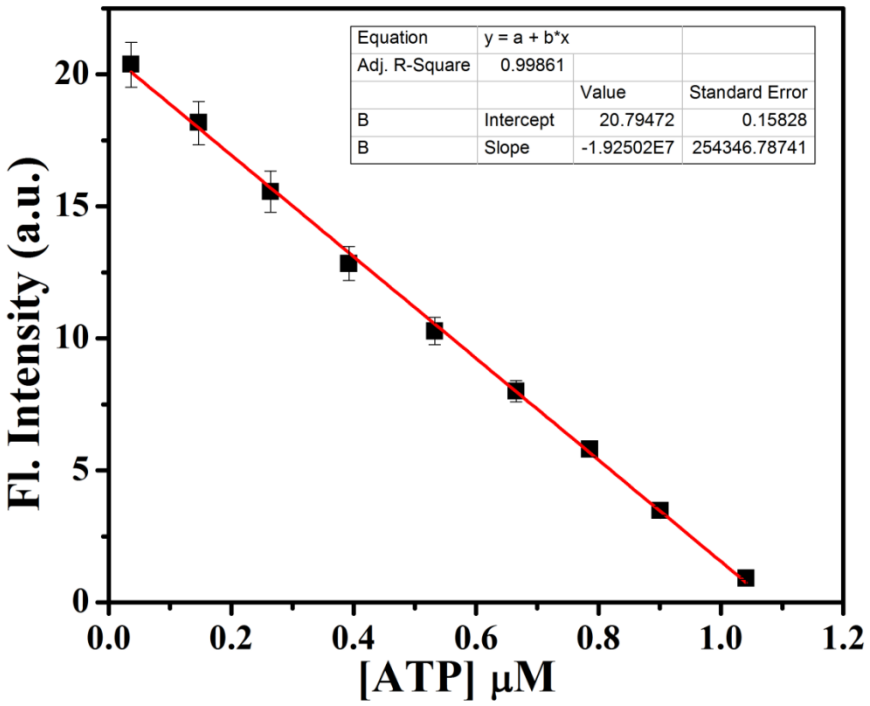

Fig. S10 Linear fit curve of **NPAC-Zn^{2+}** at 445 nm with respect to ATP concentration. Standard deviations are represented by error bar (n=3).

From the linear fit graph we get slope = 1.92502×10^7, and SD value is 0.24959

Thus using the above formula we get the Limit of Detection = 0.39×10^{-7} M, i.e 39 nM. Therefore, **NPAC-Zn^{2+}** can detect ATP up to this very lower concentration by fluorescence technique.

10. Job's plot for NPAC-Zn^{2+} complex determining the binding stoichiometry towards ATP by fluorescence method:

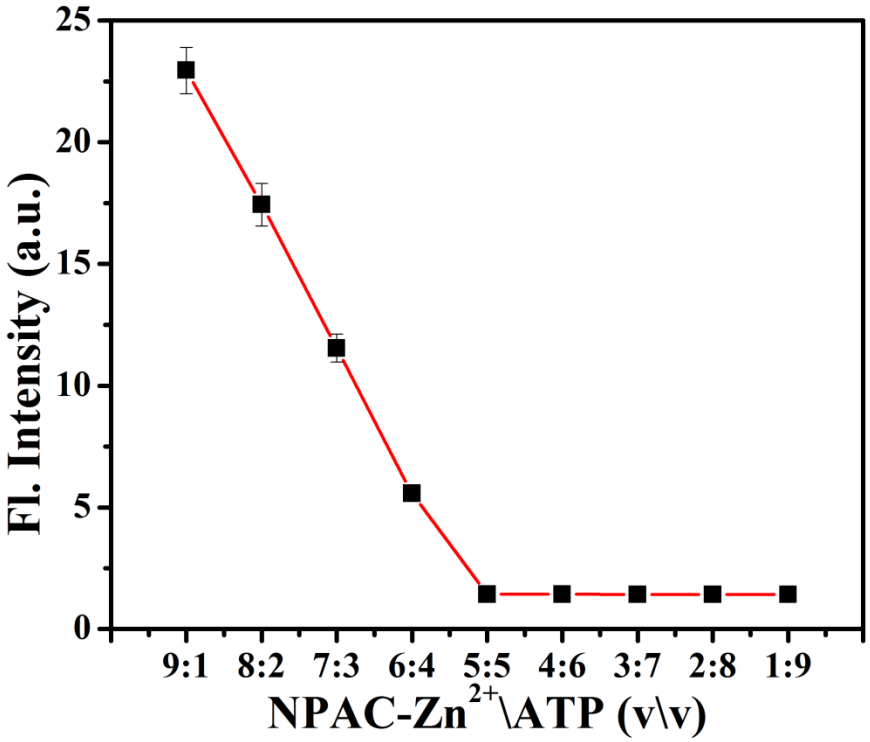

Fig. S11 Job's plot of **NPAC-Zn^{2+}** (c =1 μM) with ATP (1 μM) in acetonitrile-water (1:9, v/v) at neutral pH (pH 7.0, 10 mM phosphate buffer) by fluorescence method, which indicate 1:1 stoichiometry for **NPAC-Zn^{2+}** complex with ATP. Standard deviations are represented by error bar (n=3).

11. Competitive fluorescence studies of NPAC with different metal ions:

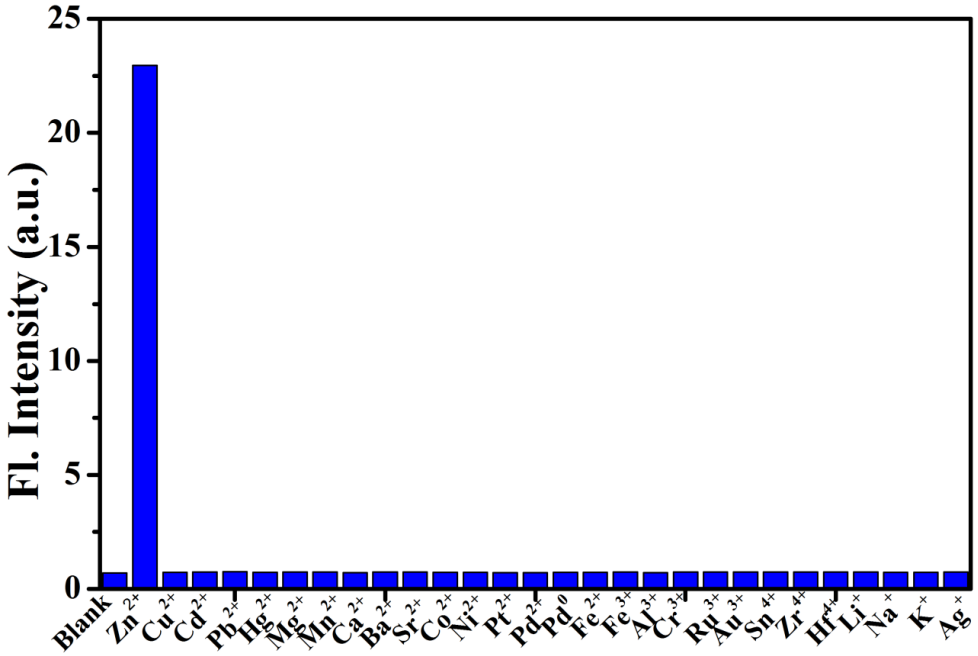

Fig. S12 Histogram representing competitive fluorescence spectra of **NPAC** with different metal ions at 445 nm (λ_{ex}= 350 nm) in CH_3CN-H_2O (1:9, v/v) at neutral pH (pH 7.0, 10 mM phosphate buffer).

12. Competitive fluorescence studies of NPAC-Zn^{2+} complex with various nucleotides and biological phosphates

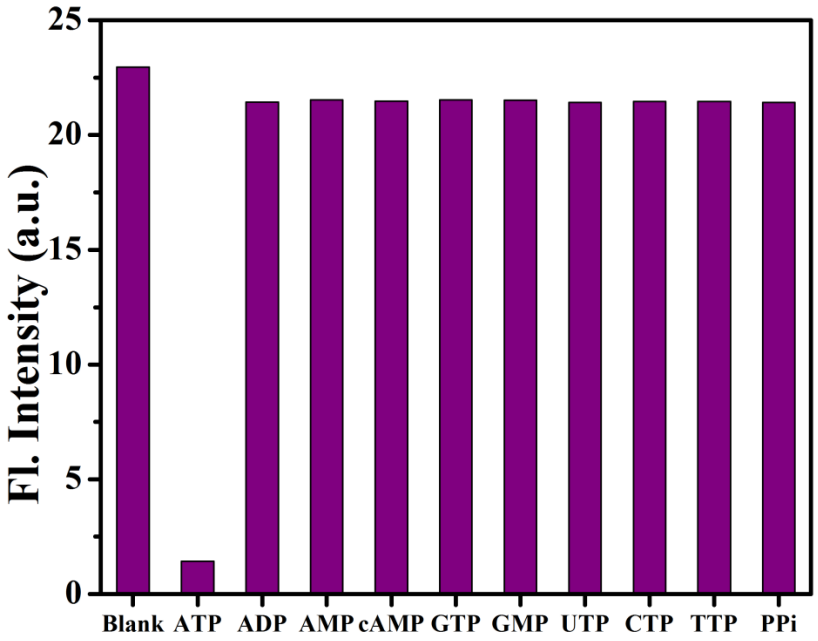

Fig. S13 Histogram representing competitive fluorescence spectra of **NPAC-Zn^{2+}** complex with various nucleotides and biological phosphates at 445 nm (λ_{ex}= 350 nm) in CH_3CN-H_2O (1:9, v/v) at neutral pH (pH 7.0, 10 mM phosphate buffer).

13. pH titration curve of NPAC upon addition of $Zn^{2+}$and NPAC-Zn^{2+} complex upon gradual addition of ATP:

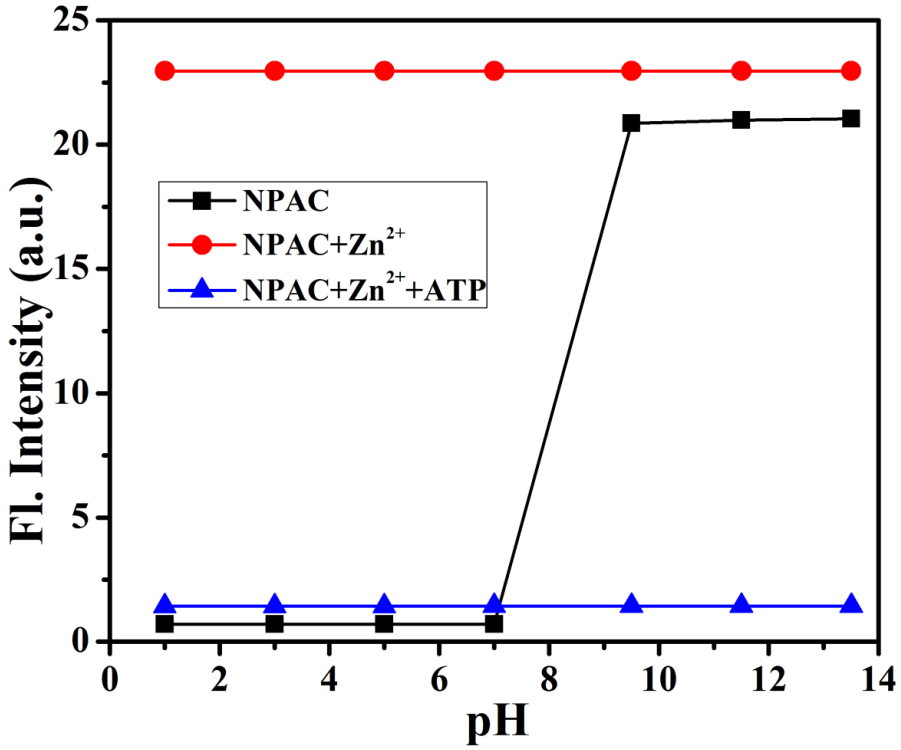

Fig. S14 Effect of pH on the fluorescence intensity of **NPAC** (1 μM) in the absence of Zn^{2+} (black line) and in the presence of Zn^{2+} (10 μM, red line) and effect of pH on the fluorescence intensity of **NPAC-Zn^{2+}** complex in the presence of ATP (blue line).

14. Details of energy calculations using Density Functional Theory (DFT):

Binding of **NPAC** with Zn^{2+} and **NPAC-Zn^{2+}** with ATP has been investigated by quantum chemical calculations at the DFT level LANL2DZ/6-31G** method basis set implemented at Gaussian 09 program. Solvent effects were incorporated using CPCM solvent model.

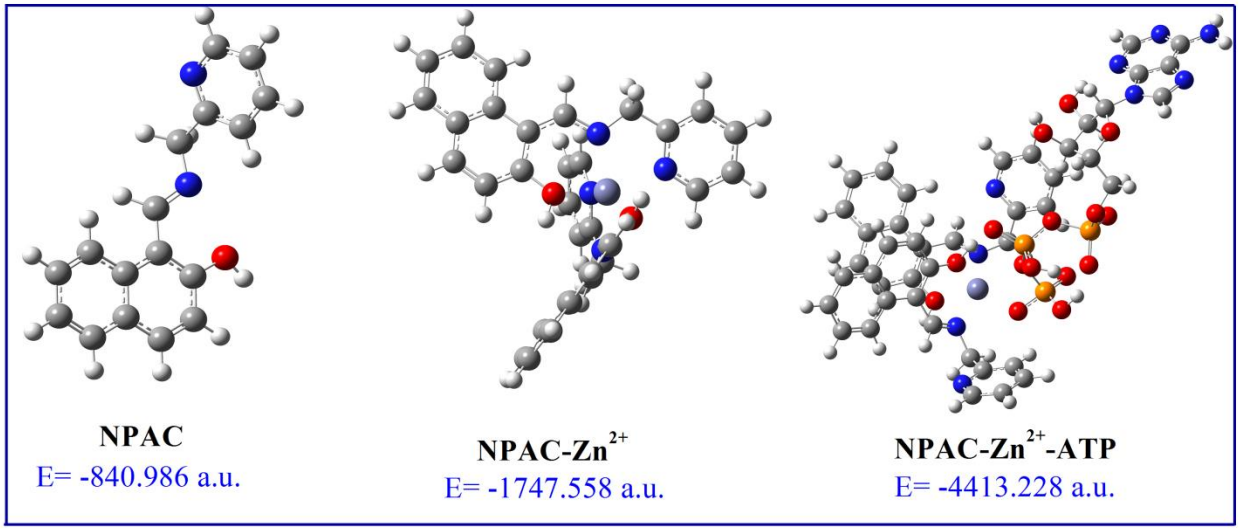

Fig. S15 Energy optimized geometries of **NPAC, NPAC-Zn^{2+}, NPAC-Zn^{2+}-ATP** and obtained at the LANL2DZ /6-31G** levels of theory with CPCM solvation (H_2O).

Table S1. Details of the geometry optimization in Gaussian 09 program.

Details	**NPAC**	**NPAC-Zn^{2+}**	**[NPAC-Zn^{2+}]-ATP**	**ATP**
Calculation method	B3LYP	B3LYP	B3LYP	B3LYP
Basis set	6-31G**	6-31G**	6-31G**	6-31G**
E(CAM-B3LYP) (a.u.)	-840.986	1747.558	-4413.228	-2666.779
Charge, Multiplicity	0, 1	2, 2	2, 2	0, 1
Solvent (CPCM)	Water	Water	Water	Water

Table S2. Selected electronic excitation energies (eV), oscillator strengths (f), main configurations of the low-lying excited states of all the molecules and complexes. The data were calculated by TDDFT//B3LYP/6-31G(d,p) based on the optimized ground state geometries.

Molecules	Electronic Transition	Excitation Energy[a]	f[b]	Composition[c] (%)

NPAC	$S_0 \rightarrow S_1$	3.8187 eV 324.68 nm	0.2348	H → L (68.7%)
	$S_0 \rightarrow S_3$	4.3030 eV 288.13nm	0.0431	H-1 → L (29%)
[NPAC-Zn^{2+}]	$S_0 \rightarrow S_{12}$	3.1439 eV 394.37 nm	0.1510	H-1 → L (58.9%)
	$S_0 \rightarrow S_{17}$	3.8206 eV 324.51nm	0.0581	H-2 → L (20%)
[NPAC-Zn^{2+}]-ATP	$S_0 \rightarrow S_4$	3. 6316 eV 341.40 nm	0.1854	H-1 → L+1 (69.6%)
	$S_0 \rightarrow S_6$	3.9301 eV 315.48 nm	0.0668	H-3 → L (19%)

[a]Only selected excited states were considered. The numbers in parentheses are the excitation energy in wavelength. [b]Oscillator strength. [c]H stands for HOMO and L stands for LUMO.

Table S3. Energies of the highest occupied molecular orbital (HOMO) and lowest unoccupied molecular orbital (LUMO)

Species	E_{HOMO} (a.u.)	E_{LUMO} (a.u.)	ΔE(a.u.)	ΔE(eV)	ΔE(kcal/mol)
NPAC	-0.21174	-0.05526	0.15648	4.26	98.19
[NPAC-Zn^{2+}]	-0.19886	-0.06813	0.13073	3.56	82.03
[NPAC-Zn^{2+}]-ATP	-0.22801	-0.07609	0.15192	4.13	95.32

15. Live Cell Imaging:

Cell line and cell culture

Cell culture: HuH7 cell lines were prepared from continuous culture in Dulbecco's Modified Eagle's Medium (DMEM, Sigma Chemical Co., St. Louis, MO) supplemented with 10% fetal bovine serum (Invitrogen), penicillin (100 µg/mL), and streptomycin (100 µg/mL). Cells were initially propagated in 75 cm^2 polystyrene, filter–capped tissue culture flask in an atmosphere of

5% CO_2 and 95% air at 37°C in CO_2 incubator. When the cells reached the logarithmic phase, the cell density was adjusted to 1.0×10^5 per/well in culture media. The cells were then used to inoculate in a glass bottom dish, with 1.0 mL (1.0×10^4 cells) of cell suspension in each dish. After cell adhesion, culture medium was removed. The cell layer was rinsed twice with phosphate buffered saline (PBS) (pH 7.0), and then treated according to the experimental need.

Cell Imaging Study: For Fluorescence imaging studies, 1×10^4 HuH7 cells in 1000 μL of medium, were seeded on sterile 35 mm glass bottom culture dish (ibidi GmbH, Germany), and incubated at 37°C in a CO_2 incubator for 10 hours. Then cells were washed with 500 μL DMEM followed by incubation with the **NPAC** (1μM) dissolved in 1000 μL DMEM at 37°C for 1 h in a CO_2 incubator and cells were washed thrice with phosphate buffered saline (PBS) (pH 7.0) to remove excess **NPAC** observed under an Olympus IX71 fluorescence microscope. Images obtained through section scanning were analyzed by DAPI filter with excitation at 339 nm monochromatic laser beams, and emission spectra were integrated over the range 459 nm. The cells were again incubated with Zn^{2+} (10μM) for 20 min and excess Zn^{2+} was washed thrice with PBS (pH 7.0).Images were captured under microscope using DAPI filter with excitation at 339 nm monochromatic laser beams, and emission spectra were integrated over the range 459 nm. The cells were again incubated with ATP (10μM) for 20 min and excess ATP was washed thrice with PBS (pH 7.0) Images were captured under microscope using DAPI filter with excitation at 339 nm monochromatic laser beams, and emission spectra were integrated over the range 459 nm For all images, the fluorescence microscope settings, such as transmission density, and scan speed, were held constant to compare the relative intensity of intracellular fluorescence.

16. Cytotoxicity Assay

In vitro studies established the ability of the **NPAC-Zn^{2+}** complex to detect ATP in biological system with excellent selectivity. Human cancer cell HuH7 were used as models. To materialize this objective, it is a prerequisite to assess the cytotoxic effect of **NPAC**, **NPAC-Zn^{2+}** and **NPAC-Zn^{2+}-ATP** complex on live cells. The well-established MTT assay[3] was adopted to study cytotoxicity of above mentioned complexes at varying concentrations. A cytotoxicity measurement for each experiment shows that the **NPAC** does not have any toxicity on the tested human cancer cell HuH7 and **NPAC-Zn^{2+}**, **NPAC-Zn^{2+}-ATP** complex does not apply significant effect on cell viability at tested concentrations.

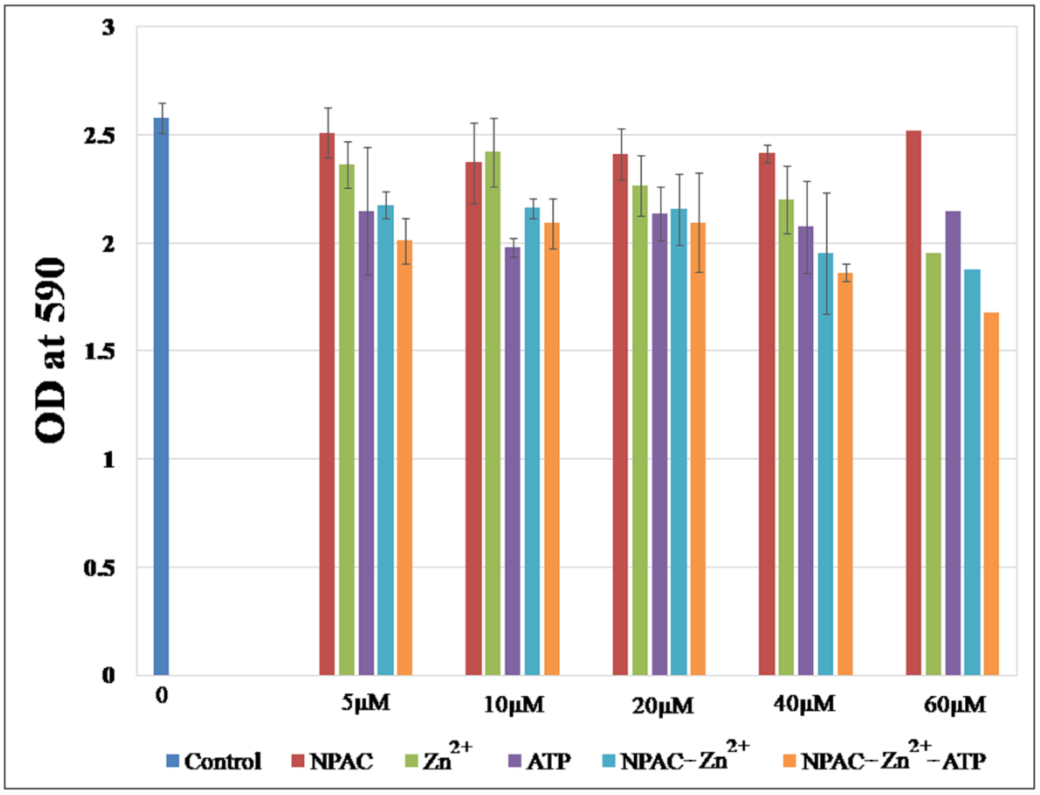

Fig. S16 MTT assay to determine the cytotoxic effect of **NPAC**, **NPAC-Zn^{2+}**, **NPAC-Zn^{2+}-ATP** complex on HuH7 cells (Human cancer cell HuH7).

17. Quantification of ATP in human cancer cells:

To quantify cellular level of ATP 10^7 HuH7 human cancer cells were harvested by centrifugation at 3000 rpm for 5 minutes followed by washing of the cell pellet with PBS buffer. Cells were again harvested following similar centrifugation. Cell pellets were suspended with 100 µL ice cold deionized water in order to lyse by the osmotic shock. Lysates were further centrifuged and the supernatant has been collected. 1 µL of supernatant has been added with the **NPAC-Zn^{2+}** (1 µM) and the fluorescence signal was measured. The value of fluorescence intensity has been plotted to the standard curve in order to know the concentration of ATP in tested samples. All estimations have been done in triplicate (Table S4).

18. Validation of the screening procedure:

The estimation of ATP was validated using different samples of HuH7 cancer cells. 10^4 of each cell suspension were centrifuged to collect the cells. The cells were resuspended with 10 mM PBS buffer (pH 7.0) followed by centrifugation. The cell pellets were lysed by osmotic shock with 1ml ice cold deionised water. 1μL supernatant were added with 1μM **NPAC-Zn^{2+}** complex and fluorescence signal were recorded. The fluorescence signal has been recorded for three independent samples of HuH7 cancer cells and all experiments were done in triplicate. The signal to noise ratio were obtained and the screening procedure were validated by calculating Z' score.

Table S4: Optimization and validation of the screening procedure for ATP level in various samples of HuH7 cancer cells using NPAC-Zn^{2+} complex

Sample	Fluorescence Intensity			Mean	Standard deviation	Signal*/Noise**	Z'
	Set 1	Set 2	Set 3				
Control	22.89	22.88	22.90	22.89	0.01	----	----
S1	3.1	3.2	3.3	3.2	0.1	0.139	0.983
S2	3.8	3.7	3.6	3.7	0.1	0.161	0.982
S3	4.0	4.1	4.2	4.1	0.1	0.179	0.982

*****fluorescence intensity for **NPAC-Zn^{2+}-ATP** interaction.

fluorescence intensity for **NPAC-Zn^{2+}complex.

All experiments were performed in compliance with the relevant laws and institutional guidelines. Institutional committee (Visva-Bharati University) has approved the experiments.

The informed consent was obtained for all experiments involving human subjects.

Reference:

[1] (a) L. Long, D. Zhang, X. Li, J. Zhang, C. Zhang and L. Zhou, *Anal. Chim. Acta.,* 2013, **775**, 100-105. (b) M. Zhu, M. Yuan, X. Liu, J. Xu, J. Lv, C. Huang, H. Liu, Y. Li, S. Wang and D. Zhu, *Org. Lett.,* 2008, **10**, 1481-1484.

[2] J. Ratha, K. A. Majumdar, S. K. Mandal, R. Bera, C. Sarkar, B. Saha, C. Mandal, K. D. Saha and R. Bhadra, *Mol. Cell. Biochem*., 2006, **290**, 113.